

Development of an innovative seismic strengthening technique for traditional load-bearing masonry walls

Jorge Proença · António Sousa Gago ·
Joaquim Cardoso · Vítor Córias · Raquel Paula

Received: 19 June 2009 / Accepted: 27 August 2010
© Springer Science+Business Media B.V. 2010

Abstract Traditional non-reinforced masonry walls are particularly prone to failure when subjected to out-of-plane loads and displacements caused by earthquakes. Moreover, singularities such as openings in façades may trigger local collapse, for either in-plane or out-of-plane motion. Bearing in mind all the former limitations, STAP, with the scientific support of ICIST and LNEC, has been developing a reduced intrusiveness seismic strengthening methodology for traditional masonry structures. The technique consists in externally applying Glass Fibre Reinforced Polymer (GFRP) composite strips to one or both faces of walls. Connection between GFRP composite strips and masonry substrate is enhanced through specifically detailed anchorages or confinement connectors. This technique has been developed and studied through an extensive series of experimental tests, which are briefly reviewed. This paper focuses more deeply on the latest experimental program, aimed at the characterization of the masonry-GFRP composite interface behaviour. This testing program comprised 29 masonry specimens, strengthened with externally bonded GFRP composite strips with anchorages. The testing variables were the number and spacing of anchorages as well as the loading history type: monotonic or repeated. Results clearly show that the use of anchorages dramatically enhances bond behaviour and that its number and spacing have a significant effect on deformation capacity and a less pronounced effect on strength. Based on experimental evidence, this paper also provides a calculation model and ULS safety assessment procedure for out-of-plane strength of reinforced masonry walls. This calculation model leads to interaction curves on strengthened masonry walls subjected to compression and out-of-plane flexure.

Keywords Masonry · Seismic strengthening · GFRP · Anchorage · Debonding · Experimental tests

J. Proença (✉) · A. S. Gago · J. Cardoso
ICIST, Civil Engineering and Architecture Department, Instituto Superior Técnico, Technical University of Lisbon, Av. Rovisco Pais 1, 1049-001 Lisboa, Portugal
e-mail: jmiguel@civil.ist.utl.pt

V. Córias · R. Paula
STAP SA, Reparação, Consolidação e Modificação de Estruturas, S. A., Lisbon, Portugal

1 Introduction

More than half of Lisbon's building stock is made up of old buildings, with load-bearing stone masonry walls. According to the 2001 Portuguese Census, only 37.8% of the Lisbon buildings have a reinforced concrete or steel structure (CML 2005), indicating that Lisbon's building stock was mostly erected before 1950. Two typologies of old masonry buildings can be found in Lisbon: the "Pombalino" type, built during the city reconstruction after the Great Lisbon Earthquake of 1755; and the "Gaioleiro" type, built in the first decades of twentieth century, during the urban growth of Lisbon.

The reconstruction of Lisbon downtown after the 1755 earthquake was conceived with earthquake resistant purposes by Manuel Damaia, Eugénio dos Santos and Carlos Mardel, all of which were engineers. Regular and symmetric building blocks with inner yards were built with the so-called "Pombalino" buildings, also inherently symmetric in plan. The structure of those buildings is composed by peripheral stone masonry walls (with rubble limestone and lime mortar) connected to a set of internal orthogonal masonry shear walls. The internal masonry shear walls were built using an innovative inner wood bracing structure, thus increasing the strength and ductility of these walls. Unfortunately, the original eighteenth century earthquake resistant concept was subsequently adulterated through architectonic changes, by the addition of extra storeys and by the lack of maintenance, leading to an actual reduced level of seismic safety for most of the "Pombalino" buildings.

In the twentieth century urban expansion of Lisbon, the construction costs and speed constraints became the most important issues for the investors. The earthquake resistant details of the "Pombalino" construction were gradually forgotten, the assemblage of internal orthogonal shear walls with wood bracing structure was discarded and the number of storeys increased, leading to an expected lower level of earthquake structural safety. Nonetheless, some characteristic elements of the "Pombalino" typology remained in the "Gaioleiro" building, such as the external stone masonry walls with rubble stone connected by lime mortar.

The generally poor constructive techniques of the "Gaioleiro" buildings, the addition of extra storeys and structural modifications carried out in "Pombalino" buildings, as well as the lack of proper maintenance in both of these buildings are the reasons for the expected high seismic vulnerability of Lisbon building stock. The awareness of this fact led STAP to the development of a strengthening technique designed specifically for Lisbon masonry buildings. An important research programme was subsequently carried out by STAP, starting with COMREHAB project (Cóias e Silva 2001), with the scientific support of ICIST (Instituto de Engenharia de Estruturas, Território e Construção, IST—TU Lisbon) and LNEC (Laboratório Nacional de Engenharia Civil—Lisbon). The present proprietary strengthening technique, consisting in externally bonded Glass Fibre Reinforced Polymer (GFRP) composite strips and mechanical anchorages, intends to improve both the out-of-plane and in-plane behaviour of stone masonry walls, increasing bending and shear strength, as well as ductility and energy dissipation capacity. This technique can be viewed as an alternative to the widely used reinforced plastering mortar technique, which consists in the application of a thin plastering mortar layer (generally placed in both sides of the masonry walls) reinforced with a steel mesh and confinement connectors.

This strengthening technique is part of a global strengthening solution for old masonry buildings, proposed by STAP. This solution comprises the reinforcement of the external masonry walls (with GFRP composite strips and anchorages—Fig. 1) together with the strengthening of the wood storey structures and the connection of these to the masonry walls (Fig. 2).

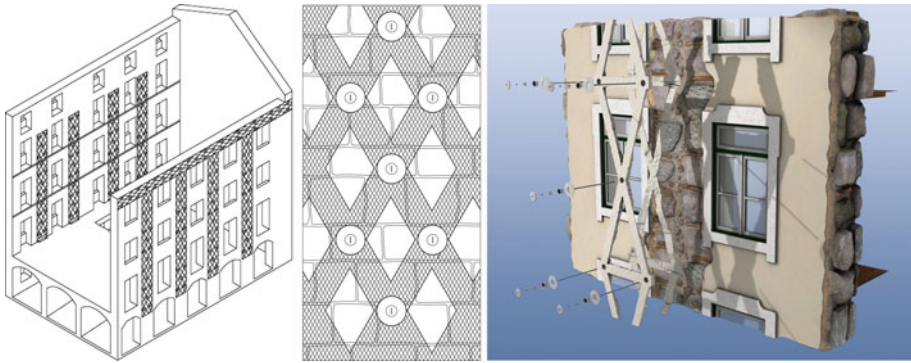


Fig. 1 View of a masonry building reinforced with GFRP composite strips and anchorages (Cóias e Silva 2007). Although less effective for out-of-plane bending, strips are depicted oriented along oblique directions, with increased benefits for in-plane shear

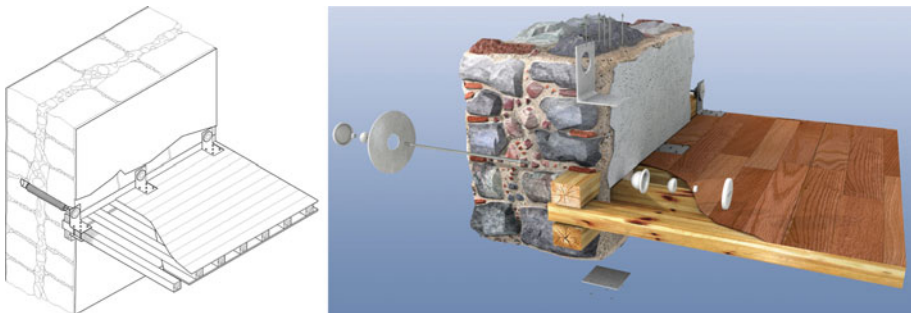


Fig. 2 Views of the “wood storey structure—masonry wall” connection, proposed by STAP (Cóias e Silva 2007)

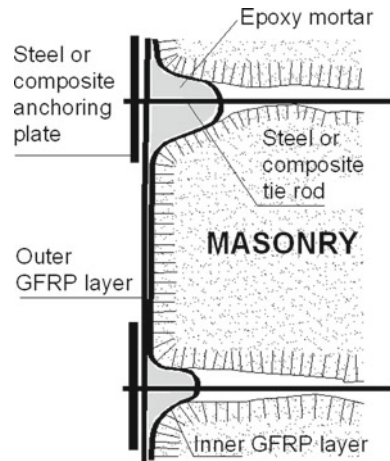
2 Description of the system under development and previous experimental studies

2.1 Description of the strengthening system

The purpose of the research programme consisted in the development of a reduced-cost strengthening technique, easy to apply, reversible and with low intrusiveness, which is a feature of particular significance in architectural heritage buildings. Due to its advantages, such as high tensile strength, low weight, non-corrosion and easy application, the composite materials, made of epoxy resin matrix, binding high resistance synthetic fibres, were chosen for the strengthening technique instead of traditional materials. Cost-effectiveness considerations dictated the choice of GFRP among other Fibre Reinforced Polymers (CFRP and AFRP). Sheet form (fabric rolls) was preferred to laminate form so that the embedment into the epoxy matrix takes place on site, allowing for the reinforcing strips to follow deliberately created grooves. The proposed strengthening technique for traditional load-bearing stone masonry walls (typically 50–80 cm thick) consists in the application of GFRP composite strips on one or, preferably, on both wall faces, connected to the masonry substrate through epoxy resin (which also forms the matrix) and mechanical anchorages.

The anchorage system prevents slip and debonding of the GFRP composite strips from the masonry substrate and increases the wall lateral confinement and, therefore, its compressive

Fig. 3 Detail of the GFRP double layer reinforcement solution and of the anchorage system (Cardoso et al. 2008)



strength. As a result, the reinforcement system has a double effect on masonry walls: increasing bending strength and ductility for out-of-plane loads; and improving shear and compressive strength, for in-plane loads.

Figure 3 depicts a typical detail. GFRP composite strips (10–20 cm wide), assembled and impregnated with epoxy resin, are applied on the wall face in two layers, connected to the masonry substrate by epoxy resin and anchorages. The anchorages, steel or composite tie rods, are placed on the wall face in drills over pre-existent or deliberately created grooves (stone joints or chiselled recesses, respectively). The first (inner) layer of GFRP is directly applied onto the masonry wall, adjusting to the shape of the groove, after which the groove is completely filled with epoxy mortar, and the second (outer) layer is stretched over the resulting flat surface. The anchoring plates, steel or composite, are then attached to the tie rods, thus compressing the grooves and the underlying masonry substrate. The working principle of the anchorage is as follows: when the masonry wall is subjected to flexure, the inner layer of the tensioned GFRP composite strip tends to straighten up, pushing the anchoring plate which is prevented from going outward by the tie rod, thus blocking the slippage of the GFRP composite strip. Despite the fact that composite anchorages and tie rods may present some advantages in terms of corrosion resistance, all reported tests were conducted with steel components.

Compared with the traditional strengthening methods for masonry walls (ACI 2007; CNR 2004; Jifu et al. 2007), this methodology presents some advantages, such as lower intrusiveness, negligible increase in mass and wall thickness, dry nature of the method (without hydraulic mortars), ease of application and non-corrosiveness of the reinforcement material.

2.2 Previous experimental studies

The development of the strengthening technique started in 1998 within the scope of the COMREHAB research project. The experimental development of the strengthening technique was divided into the following series of tests: elementary material tests, medium scale tests in both masonry specimens (compression and bending) and wall models and, finally, shaking table tests of scaled building models. Table 1 summarizes all the experimental series of tests performed to date.

Table 1 Chronological table of the previous experimental development stages

Year	Participants	Designation
1998	STAP	Development of a poor cement mortar to substitute masonry
1999	IST—STAP	Characterization and comparison of mechanical properties of common masonry specimens with mortar specimens
2000	IST—STAP	Bending tests in reinforced masonry specimens
2001	IST—STAP	Out-of-plane cyclic tests in masonry wall specimens
2001	LNEC—STAP	In-plane cyclic tests in masonry wall specimens
2004	LNEC—STAP	Experimental shaking table tests of 1:3 scale building models

Table 2 Experimental range for compressive strength (MPa) and Young's modulus (GPa) in mortar and common masonry specimens

Experimental series	Mechanical property		
	Compressive strength range (MPa)	Young's modulus range (GPa)	Number of specimens
Mortar	1.46–2.28	0.87–1.01	4
Stone masonry	0.95–1.19	0.97–1.13	6
Brick masonry	Type 1	4.99, 5.15	2
	Type 2	2.78	0.95–1.28

From the start it was evident that such an extensive test programme could hardly be accomplished with real masonry specimens. For this reason STAP proposed that all specimens were built with a poor (low amount of cement) mortar, developed so as to simulate some of the more relevant mechanical properties of common traditional masonry: compressive strength of 1.5 MPa and Young's modulus of 1 GPa in compression. Out-of-plane flexural (with vertical compression) and bonding behaviours were assumed to depend mainly on those two mechanical properties, similarly to what happens in concrete materials. The effect of irregularities, typical of stone masonry walls when the external plastering mortar is removed, is not fully simulated by this material; however this strengthening technique requires that the surface onto which the GFRP composite strips are to be applied to be smoothed (through a thin plastering mortar layer) rendering all irregularity similitude concerns irrelevant. The smoothing of the masonry wall faces also eliminates direct contact between GFRP and stone blocks, rendering the GFRP-stone adhesion similitude concerns also irrelevant. The mix retained for subsequent developments was chosen within a set of different mixes with different proportions of cement, hydraulic lime, aggregates (fine and coarse), concrete additives and water. In 1999, the compressive strength and Young's modulus were experimentally measured for three real masonry series of specimens (one series of stone masonry specimens and two other series of brick masonry specimens). These real masonry mechanical properties were subsequently considered as references for the validation of the chosen type of mortar mix that evolved from those initially studied in 1998 (Table 2).

Bending tests in mortar wall specimens (cross section of $0.60 \times 0.20 \text{ m}^2$, span of 1.10 m) consisted in the first attempt to measure the anticipated out-of-plane benefits of this strengthening technique. These mock-up masonry specimens had grooves to simulate pre-existent real masonry surface joints or deliberately-made grooves to increase anchoring effectiveness.

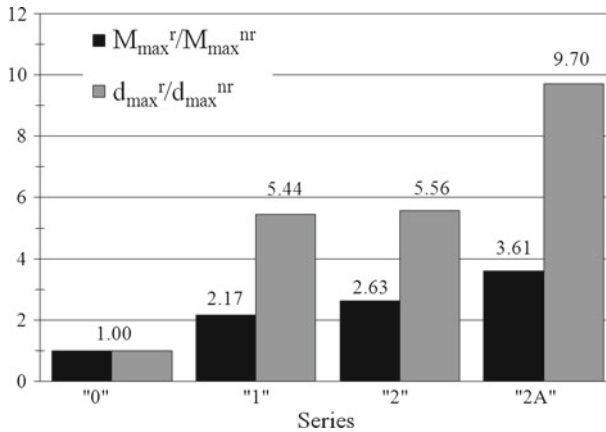


Fig. 4 Comparative efficiency of reinforced (r) versus non-reinforced models (nr) in terms of ultimate bending moment (M) and ultimate displacement (d). Series “0”, non-reinforced, Series “1”, GFRP composite strips only in tension face; Series “2”, GFRP composite strips in both faces; and Series “2A”, GFRP composite strips in both faces with anchoring devices and grooves

The experimental models database included four types of masonry specimen series, depending on the reinforcement type: non-reinforced (series “0”), GFRP composite strips only in tension face (series “1”), GFRP composite strips in both faces (series “2”), and GFRP composite strips in both faces with anchoring devices and grooves (series “2A”). Figure 4 shows the relative efficiency of the strengthened specimens in terms of both strength and deformation ability.

Since 2001, the experimental development stages were divided into the study of the out-of-plane and the in-plane behaviour of strengthened masonry wall models. ICIST and LNEC were, in that order, assigned the out of plane and in-plane experimental programmes.

Out-of-plane behaviour was studied through 12 masonry wall specimens, varying the type of reinforcement, identified as previously in four series: “0”, “2”, “2A” and “2A*” (same as “2A” but without grooves), each of these series consisting of 3 identical specimens. These wall specimens presented the following external dimensions: 2470 mm (height) \times 1700 mm (width) \times 220 mm (thickness). The cross section width of the wall was decreased to 1250 mm along an intermediate height of 1560 mm, so that damage would concentrate in this critical zone. In specimens with grooves—series “2A”—the thickness of the specimens was further reduced to 170 mm along grooves (25 mm deep grooves in both faces).

The main objective of the experimental campaign carried out at ICIST was to compare the cyclic performance of each strengthening technique by imposing an out-of-plane reversed cyclic horizontal displacement history to the masonry wall specimens. In addition, a constant normal force was applied to the top of the wall producing a 0.66 MPa constant vertical compressive stress (simulating the effect of both live and dead loads in real wall structures). Figure 5 illustrates the experimental setup. The hydraulic jacks shown on one face applied a constant vertical compressive force through pre-stressing tendons anchored at the top of the specimen, whereas the actuator (on the background) imposed a reversed cyclic out-of-plane displacement history. This loading history consisted in single alternate drift cycles of 0.15, 0.30, 0.45%, followed by series of three alternate drift cycles of 0.6, 1.2, 1.8, 2.4, ..., with 0.6% (10 mm) increments, until failure occurred.

Fig. 5 Out-of-plane experimental campaign. Experimental setup

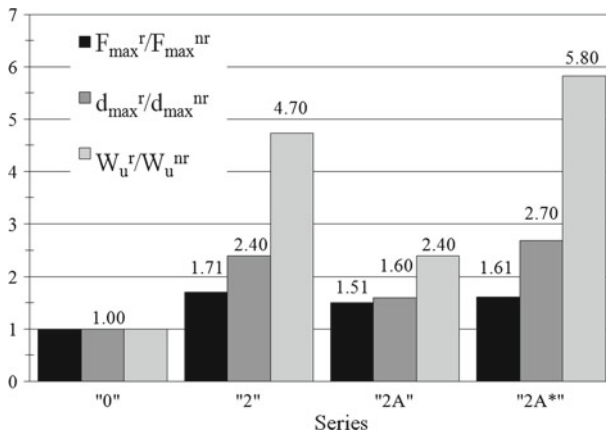


Fig. 6 Comparative efficiency of reinforced (r) versus non-reinforced models (nr) in terms of maximum force (F_{max}), ultimate displacement (d) and accumulated dissipated energy at collapse (W_u). Series "0", non-reinforced; Series "2", GFRP composite strips in both faces; Series "2A", GFRP composite strips in both faces with anchoring devices and grooves; and Series "2A*", GFRP composite strips in both faces with anchoring devices but without grooves

The out-of-plane experimental campaign results can be summarized comparing the maximum force (F_{max}) and ultimate displacement (d_u), as well as the accumulated dissipated energy at collapse (W_u). Figure 6 shows the average values of the former indicators, computed for each of the series with respect to series "0" (non-reinforced).

The presence of anchorages, or the way they were applied in series "2A", may have had a detrimental effect when these tests are compared to series "2", as shown by the decrease of the indicators. This detrimental effect is probably due to stress concentrations resulting from the wall thickness reduction near the grooves. The fact that in models "2A*" the decrease of these indicators is practically inexistent further substantiates the previous conclusion.

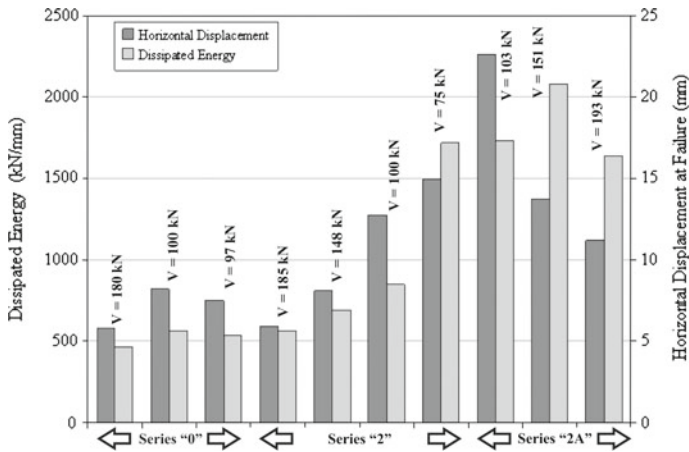


Fig. 7 Horizontal displacement and dissipated energy at failure, depending on reinforcement technique and compression level (V —Vertical compression force). Series “0”, non-reinforced; Series “2”, GFRP composite strips in both faces; and Series “2A”, GFRP composite strips in both faces with anchoring devices and grooves

The in-plane testing campaign, assigned to LNEC (Campos-Costa et al. 2001), was composed by a total of 10 specimens with dimensions identical to those of the out-of-plane specimens. The testing setup was also comparable to that of the former testing campaign—vertical jacks and pre-stressing tendons to ensure a constant vertical compression force and horizontal displacement imposed at the top of the masonry wall specimen through an actuator—with the difference that the actuator motion was in the plane of the wall. Three series of specimens were considered—“0”, 3 specimens, “2”, 4 specimens, and “2A”, 3 specimens. These 3 series of specimens were manufactured in different occasions (one for each series) with 3 different mortar batches, although, theoretically, with the same mortar mix. In this testing campaign the constant vertical compression force was considered also as a variable, varying within each of the former 3 series of specimens.

At an equivalent compression level, the benefits of this strengthening technique can be clearly inferred by observing Fig. 7, which summarizes the horizontal displacement and the accumulated dissipated energy, both at failure, for all specimens (the vertical compression force for each test, V , is also shown in that figure). These benefits are clearly more evident for specimens of series “2A” due to the lateral confinement of masonry provided by the GFRP composite strips (and anchorages) and also because the existence of anchorages was shown to prevent a premature failure mode consisting in GFRP debonding.

Apart from confirming the advantages of the strengthening technique, this testing campaign allowed for the study of its effectiveness in increasing the in-plane deformation capacity of the walls for varying levels of compression force. This beneficial feature can be expressed in terms of the maximum allowable drift (ratio between the in-plane displacement at failure and the deformable height) versus axial force ratio ν (vertical compressive stress divided by the crushing strength), as shown in Fig. 8. For some reason, the average crushing strength corresponding to specimens of series “2A” was much lower than those of the other series. Considering that the range of vertical forces was of similar magnitude for all series of specimens, the former disturbance led to axial load ratios much higher for series “2A” than those of series “0” and “2”. With this limitation in mind, isolated plot values—each corresponding to a different test—seem to indicate that drift relates to axial force ratio in a consistent manner

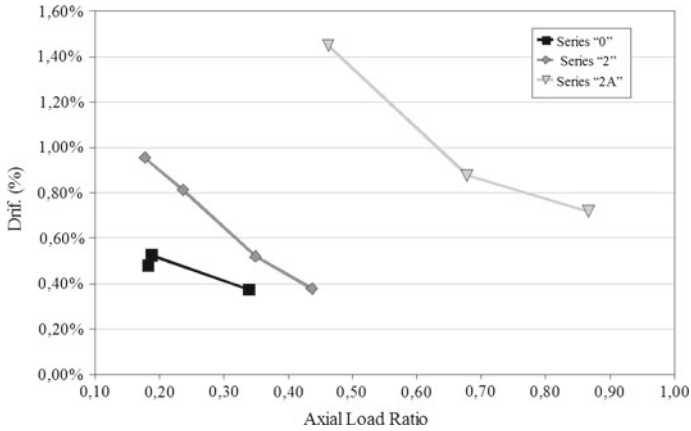
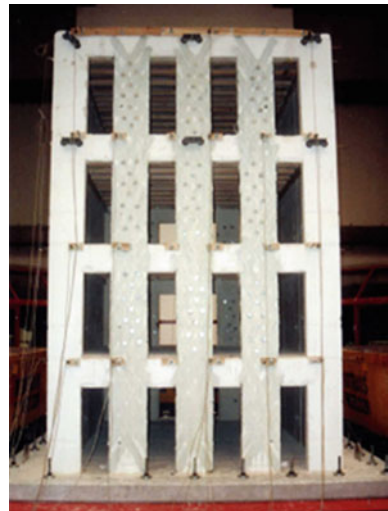


Fig. 8 Results from in-plane tests: axial load versus drift (data from Campos-Costa et al. 2001). Series “0”, non-reinforced; Series “2”, GFRP composite strips in both faces; and Series “2A”, GFRP composite strips in both faces with anchoring devices and grooves

Fig. 9 Façade of the model reinforced with GFRP and anchoring devices (Candeias et al. 2004)



for each of the strengthening techniques (including non strengthened specimens) and that the increase in the axial force ratio decreases the available drift.

Prior to the bonding test programme, described in Sect. 3, the more recent developments of the strengthening technique consisted in shaking table tests of 1:3 geometrically scaled building models, initiated in 2004. This testing programme was performed under the scope of MITRIS research project (Candeias et al. 2004, 2006) and comprised shaking table tests of 5 building models with different strengthening techniques (or combination of these). One of these building models, shown in Fig. 9, was strengthened according to this technique (“2A” version, with added in-floor steel ties) and withstood without collapsing a ground motion history conforming to the Lisbon’s 1755 earthquake (estimated magnitude of 8.5). Maximum Peak Ground Acceleration (PGA) values of 1 g (9.8 m/s²) were imposed to the model,

which, considering similitude laws, corresponds to PGA values of 0.33 g (3.27 m/s^2) in the prototype.

3 Experimental bonding tests programme

The flexural behaviour of stone masonry walls strengthened with externally bonded and anchored GFRP composite strips is highly influenced by the effectiveness of the GFRP-Masonry Substrate interface. Consequently, the assessment of the most influential bonding factors, and their effects on an out of plane design model for strengthened masonry walls, was the main objective of the experimental programme. A total number of 29 masonry specimens were tested in this programme. These specimens were cast with the special mortar which reproduces the compressive strength, elasticity modulus and, presumably, bonding characteristics of traditional stone masonry walls.

3.1 Materials

The experimental programme started with the mechanical characterization of mortar and GFRP composite strips. Compressive tests on mortar-masonry cubic specimens (150 mm side), performed according to the Portuguese national standard LNEC E226 (LNEC 1993), indicated an average compressive strength of 1.30 MPa. Tensile tests were performed on 6 GFRP composite strip specimens (3 single-layer, SL, and 3 double-layer, DL) and the results are summarized in Table 3. Tests on GFRP composite strips were performed according to the following ISO standards: 527-1 (ISO 1993), 527-4 (ISO 1997a) and 527-5 (ISO 1997b).

When the mechanical characteristics are computed based solely on the fibre cross section two seemingly contradictory effects arise: the elastic modulus is about the double of that of the manufacturer data for virgin filaments ($E_f = 65 \text{ GPa}$), whereas the maximum strength is about half of the manufacturer value ($\sigma_{fu} = 3 \text{ GPa}$). The first effect can be explained by the fact that the contribution of the epoxy matrix is neglected, leading to an over estimation of the fibre stress. Despite that, the detrimental consequences due to the inclusion of the fibre in the matrix are such that the maximum fibre stress, computed in the same way, falls significantly below the manufacturer specifications for filaments (second effect). All these

Table 3 Results from tensile tests on GFRP composite strips

Specimen	Fibre cross section mm^2	Composite cross section mm^2	Elastic Modulus (GPa) E_f based on		Tensile strength (MPa) σ_{fu} based on	
			Fibre cross section	Composite cross section	Fibre cross section	Composite cross section
SL1	7.45	74.25	117.45	11.78	1630.87	163.64
SL2	7.45	80.00	116.78	10.88	1759.73	163.88
SL3	7.45	85.00	124.83	10.94	1761.07	154.35
Average			119.69	11.20	1717.23	160.62
DL 1	14.90	125.00	134.56	16.04	1275.84	152.08
DL 2	14.90	126.25	122.15	14.42	1357.05	160.16
DL 3	14.90	123.25	107.05	12.94	1448.32	175.09
Average			121.25	14.47	1360.40	162.44

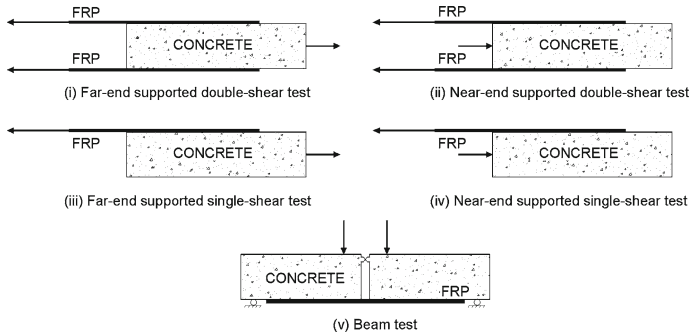


Fig. 10 Configurations for bond tests (Chen et al. 2001)

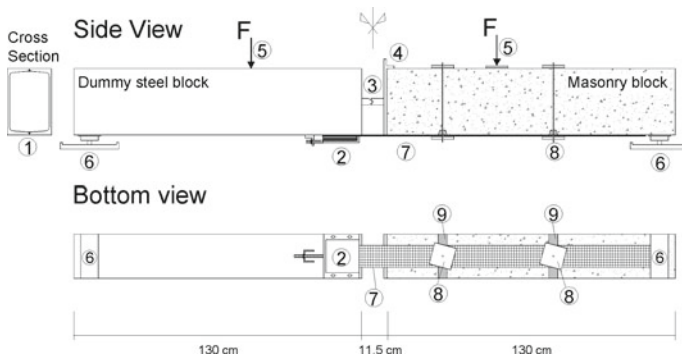


Fig. 11 Test configuration (*side and bottom views, masonry block on the right*) (Gago et al. 2009). *Legend:* 1 2 UNP 300, 2 fibre anchoring device, 3 compression hinge, 4 steel plate, 5 applied force, 6 vertical support, 7 composite GFRP composite strip, 8 anchorage or confinement connector (steel plate + steel tie rod), 9 groove

conclusions are in line with either the well known “rule of mixtures” (FIB 2001) or the manufacturer design recommendations (S&P 2002) (consideration of the fibre cross section and cumulative reduction of the strength by a design factor of 1.5–1.8).

3.2 Test configuration

Different test configurations (Kiss et al. 2002a; Chen et al. 2001) have been used in the past to study the stress distribution and deformation along the bonded length, as shown in Fig. 10.

The test setup adopted for the present study resulted from modifications carried out on the “beam test” configuration, which originally implies the use of two blocks per test. One of these modifications, aiming at the reduction of the total number of masonry blocks, consisted in the use of a dummy steel block, the same in all tests, leading to a single masonry block being damaged at each test (Fig. 11). These tested blocks, henceforth referred to as “masonry blocks”, are made of equivalent mortar masonry material as described previously.

Another modification consisted in the location of the compression hinge at mid-height of the specimen cross section ($20 \times 30 \text{ cm}^2$, length 130 cm). Except for a rigid body rotation, the setup is similar to the “single-shear” configuration, with a state of pure tension in GFRP. Figure 12 shows the test setup and the steel frame assembled for the present experimental programme.

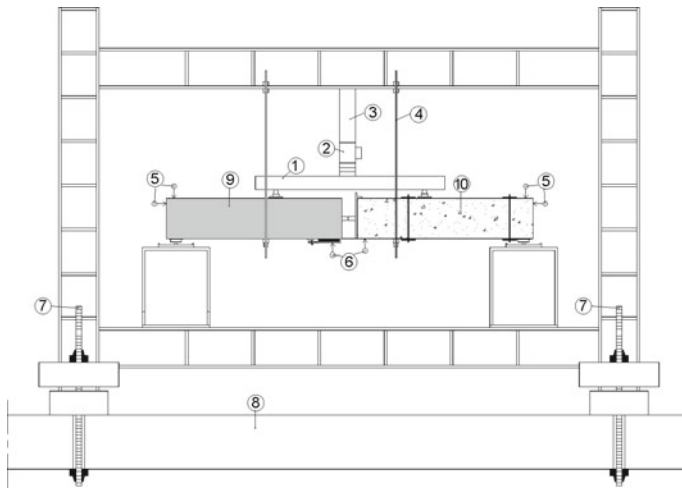
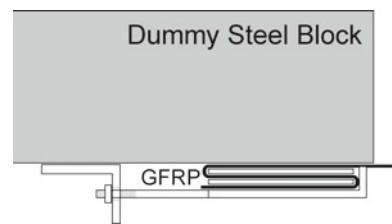


Fig. 12 Test setup (side view). Legend: 1 load distribution beam, 2 load cell, 3 hydraulic jack, 4 provisional hanging system, 5/6 displacement transducers, 7 dywidag bar, 8 stiff floor, 9 dummy steel block, 10 masonry block

Fig. 13 Detail of fibre anchoring device in steel block. (Cardoso 2008)



3.3 Test loading procedure

Testing procedure was as follows: (i) release of the provisional hanging system, activating the fibre tensile stresses to balance the self weight of the blocks; (ii) stepped loading, monotonic or cyclic (repeated with increasing force amplitude), through the hydraulic jack and the distribution beam.

3.4 Masonry specimens

Masonry specimens were reinforced with 10 cm wide GFRP composite strips and anchorages, following the described methodology. A special GFRP composite strip anchoring device on the dummy block was conceived for the testing programme (Fig. 13). The anchorage procedure consisted in folding the composite strip (before hardening) around two steel plates and clamping this set with adjustable bolts.

Considering that the existence and detailing of anchorages is a distinctive feature of the strengthening technique, a total number of 29 reinforced specimens were tested, with different numbers of anchorages (1 or 2) and spacing (25, 50 or 75 cm). Masonry specimens were divided into six general series, one for each anchorage spacing/number combination (Table 4). The identification of each specimen was as follows: a specimen with “n” anchorages, spaced “s” centimetres is designated by Ms-n-120, where the number 120 indicates the fibre bonded

Table 4 Specimen identification and characteristics

Spacing between anchorages	Number of anchorages	Series name	Loading type	Number tests	Test name
25 cm	1	M25-1	Monotonic	3	M25-1-120 (M1 to M3)
			Cyclic	1	M25-1-120 (C1)
	2	M25-2	Monotonic	2	M25-2-50 (M1 and M2)
			Cyclic	3	M25-2-120 (M3 to M5)
50 cm	1	M50-1	Monotonic	3	M50-1-120 (M1 to M3)
			Cyclic	1	M50-1-120 (C1)
	2	M50-2	Monotonic	3	M50-2-120 (M1 to M3)
			Cyclic	1	M50-2-120 (C1)
75 cm	1	M75-1	Monotonic	3	M75-1-120 (M1 to M3)
			Cyclic	1	M75-1-120 (C1)
	2	M75-2	Monotonic	4	M75-2-120 (M1 to M4)
			Cyclic	1	M75-2-120 (C1)
	0	M120	Monotonic	1	M120 (M1)

length (in cm). The location of the first, innermost, anchorage is dictated by anchorage spacing; this first anchorage is located at a distance from the innermost free end of the masonry block equal to half of the anchorage spacing (so that if the dummy block was replaced by another equivalent masonry block, anchorage spacing would remain constant throughout the two blocks). Each series generally comprised four specimens, of which three were subjected to monotonic loading (suffix M) and the fourth was subjected to cyclic, repeated, loading (suffix C). The loading history was as described: monotonic tests—increasing load with 1 kN increments until collapse; cyclic tests—repeated cycles with increasing amplitude starting and ending at 1–2 kN (1 cycle), 3 kN (1 cycle), 4 kN (3 cycles), 7 kN (3 cycles), 10 kN (3 cycles), 13 kN (3 cycles),..., until collapse. One control specimen, without anchorages, was further tested to assess the beneficial effects of the anchorages. This specimen—M120 (M1)—was tested to confirm that the possibility of taking due advantage of the GFRP high tensile strength relies on the anchorage effect and that composite strip-masonry bonding strength is comparatively low. As previously shown in Fig. 12, the instrumentation comprised a load cell, six displacement transducers (to measure the block rotation). Although not shown in Fig. 12, strain gauges were also placed on the GFRP composite strip in different locations along its length: one in the beam mid-span, one for each anchorage position and one for each of the segments between anchorages.

3.5 Experimental tests

The experimental programme started with a monotonic loading test on the M75-2-120 (M1) specimen, reinforced with a bidirectional glass fabric with a longitudinal fibre cross section of 13.00 mm² (50/50 distribution with a total weight per layer of 350 g/m²). In this test failure occurred by tensile fracture of the GFRP composite strip before the anchorage closest to the compression hinge (T failure, Fig. 14a), which showed negligible damage effects. To instigate the participation of the anchorages, the remaining specimens were strengthened with a more resistant uni-directional glass fabric (with a longitudinal fibre cross section of

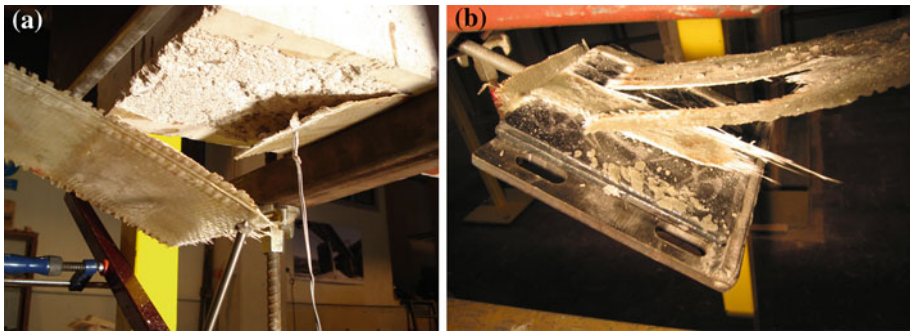


Fig. 14 (a) GFRP tensile fracture—test M75-2-120 M1 (T failure); (b) GFRP cut due to stress concentration in the edges of the anchoring device set on the dummy steel block (P₁ failure)

29.80 mm², 90/10 distribution with a total weight per layer of 440 g/m²). In the remaining tests of the series M75-2-120 (M2, M3, M4 and C1) the maximum developed stress in the GFRP (uni-directional fabric) increased, and premature failure occurred due to tear of the composite strip in contact with the sharp edges of the anchoring device set within the dummy steel block (P₁ failure, Fig. 14b). To avoid this premature failure mode, the edges of the anchoring device were subsequently smoothed and an additional GFRP layer was placed in the composite strip within this device. None of these changes had any influence on the bonding behaviour along the reinforced masonry block. The succeeding test stage corresponded to two M25-2-50 specimens, M1 and M2, with a reduced (50 cm) strip length which led to a sudden discontinuity in terms of the bending strength of the masonry block. In these two specimens premature collapse was due to flexural failure of the masonry block developing near the cross section where reinforcement was suddenly interrupted (P₂ failure, Fig. 15a). In all the remaining test specimens the GFRP composite strip was extended to a cross section near the support (120 cm long), where the bending moments are negligible. In the following tests, M25-2-120 (M3, M4, M5, C1 and C2), failure predominantly resulted from composite strip tear/fracture in the first innermost anchoring plate (A₁ failure, Fig. 15b) in the masonry block, possibly due to stress concentration near the anchoring plate, deviation force effects and stress concentration induced by the groove and anchorage. This failure mode corresponded to a better and more realistic use of the GFRP high strength fabric, resulting from increased anchorage effect. Failure of M50-1-120 and M75-1-120 specimens, reinforced with only one anchorage, occurred due to GFRP composite strip debonding along the full length and consequential damage to the anchorage system (A₂ failure, Fig. 16a). In series M50-2-120 and M75-2-120, reinforced with two anchorages, failure occurred respectively due to composite strip tear on the first innermost anchoring plate (A₁ failure) in the masonry block, and due to composite strip tear in contact with the anchoring device (P₁ failure). Specimens of series M25-1-120 collapsed by crushing of the compressed masonry strut, which developed between the first anchorage and the compression hinge (C failure, Fig. 16b). Finally, specimen M120, reinforced with no anchorages, collapsed by composite strip debonding (D failure) during the initial stage of the test, when releasing the provisional hanging system (bond strength was insufficient to balance the self weight of the blocks).

3.6 Test results

Table 5 summarizes the most relevant results of the experimental programme.

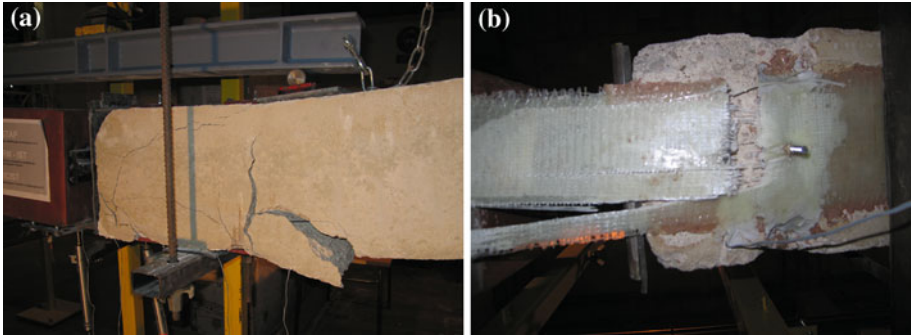


Fig. 15 (a) Flexural failure of the masonry block near the cross section where reinforcement was interrupted (P_2 failure); (b) GFRP cut on the first innermost anchoring plate (view after dismantling the anchorage system) (A_1 failure)

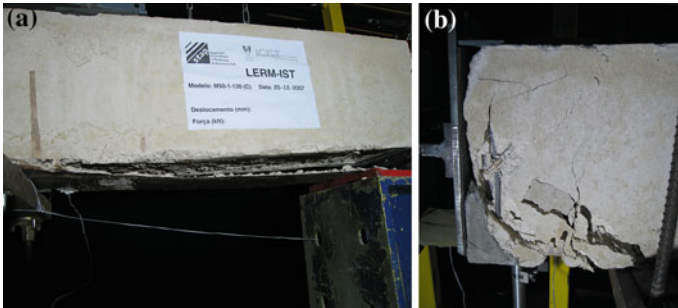


Fig. 16 (a) GFRP debonding after the anchorage (A_2 Failure); (b) Masonry crushing (C Failure)

In spite of the observation that failure can be considered premature in a significant number of tests (italicize in Table 5), the first general conclusion is that the strengthening technique is extremely effective, allowing high tensile stresses to be developed in the GFRP composite strips. These high tensile stresses are a consequence of the effectiveness of the anchoring technique and details, indirectly leading to different premature failure modes— P_1 and P_2 —that reflect limitations of the testing setup and components, rather than those of the strengthening technique. If these premature failure modes had not occurred, possibly higher stresses could have been developed in the composite strips. Even so, for most tests tensile stresses in excess of 1 GPa can be computed in the GFRP if the epoxy resin area is neglected in the calculations. Failure by masonry strut crushing (C failure) can be viewed a collateral effect of the test setup, since in the tests the resultant of compression stresses is forced to act at mid-depth (compression hinge location), whereas in real situations the resultant should be near the upper limit of the cross section and the compression strut would involve more masonry material. In M25-1, single anchorage series of specimens, this failure mode was recurrent as a consequence of the fact that the compression strut is forced to develop between the compression hinge and the first, and only, anchorage, located at only 12.5 cm from the innermost free end of the masonry block, involving less equivalent-masonry material and presenting a steep slope. Realistic failure modes are those that result either from anchorage failure (A_1 and A_2 failures) or from tensile fracture of GFRP (T failure). Maximum GFRP strain at collapse (measured by strain gauges placed on the composite strip in the beam mid-span)

Table 5 Experimental results

Series	Loading type	Number of anchorages	Spacing between anchorages (cm)	Bonded fibre length (cm)	Fibre cross Section A_f (mm ²)	Failure mode	Max. GFRP force F_u (kN)	Max. GFRP strain ε_u (‰)	
M25-1	M1	1		120	29.80	C	26.04	6.08	
	M2				29.80	C	24.00	5.43	
	M3				29.80	C	26.00	6.83	
	C1				29.80	C	38.93	12.94	
M25-2	M1	2	25	50	29.80	P_2	31.78	7.79	
	M2				29.80	P_2	28.24	6.76	
	M3				120	29.80	A_1	31.86	7.70
	M4				29.80	A_1	38.13	13.74	
	M5				29.80	P_1	34.34	13.89	
	C1				29.80	P_1	34.27	11.08	
	C2				29.80	A_1	33.26	14.61	
M50-1	M1	1		120	29.80	P_1	32.37	9.37	
	M2				29.80	A_2	32.93	9.92	
	M3				29.80	A_2	28.28	8.33	
	C1				29.80	A_2	26.06	8.37	
M50-2	M1	2	50	120	29.80	C	35.78	12.38	
	M2				29.80	A_1	38.16	11.58	
	M3				29.80	A_1	40.73	12.03	
	C1				29.80	A_1	36.04	13.34	
M75-1	M1	1		120	29.80	A_2	35.83	8.97	
	M2				29.80	A_2	28.33	9.28	
	M3				29.80	A_2	28.40	8.85	
	C1				29.80	A_2	30.70	9.86	
M75-2	M1	2	75	120	13.00	T	21.96	11.83	
	M2				29.80	P_1	36.09	8.47	
	M3				29.80	P_1	39.95	7.75	
	M4				29.80	P_1	25.90	12.49	
	C1				29.80	P_1	35.70	11.83	
M120	M1	0	∞	120	0	D	8.90		

Note (failure modes): C masonry crushing, P_2 flexural failure of the masonry block, GFRP tear fracture in the anchorage system (A_1) or in the anchoring device (P_1), A_2 GFRP debonding and consequential anchorage system damage, T GFRP tensile fracture, and D composite strip debonding

generally exceeded 8‰ in all specimens that presented realistic failure modes. The comparison of M50-1 and M50-2 series (only series where there was a significant number of non-premature failure modes) suggests that the increase in the number of anchorages is beneficial in terms of the maximum force. Double anchorage specimens generally presented higher levels of deformation capacity, due to stress redistribution between the innermost and outermost anchorages. Morsch's truss analogy, similarly to that of reinforced concrete beam shear behaviour models, in conjunction with C failure mode, suggests that anchorage spacing in the order of magnitude of the wall thickness would be advisable. In spite of that observation,

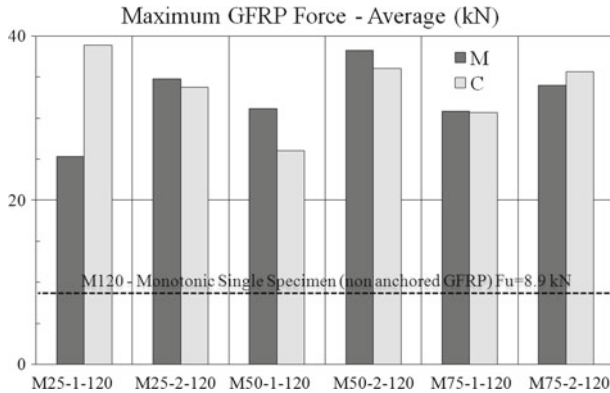


Fig. 17 Strength increase compared to the traditional reinforcement solution, without anchorages

maximum composite force showed no clear dependency on the anchorage spacing for the spacing range considered. Contrarily to what could be expected, there was no consistent decrease in strength in specimens subjected to cyclic load history. Finally, tests showed the need for anchoring the GFRP composite strip ends or to extend the GFRP laminate to zones where bending moments are negligible, thus avoiding premature debonding, and that the debonding failure mode (D) was successfully excluded in all reinforced test specimens.

Figure 17 summarizes the maximum composite force, normalized with respect to that of the specimen reinforced without anchorages. Data is presented grouping all tests according to the number, and spacing, of anchorages and loading pattern. This figure clearly shows a significant increase in strength developed in specimens with anchorages, thus proving the effectiveness of this anchoring system in taking maximum advantage of the GFRP strength.

4 Calculation model for out-of-plane behaviour

The effectiveness of the strengthening system was further studied through the development of a calculation model for the design of the strengthened walls when subjected to combined compression and out of plane flexure. This model is based on the following assumptions (Yao et al. 2005; Kiss et al. 2002b; Tumialan et al. 2003):

- Bernoulli's hypothesis (plane sections remain plane);
- Full adherence hypothesis (same strain in GFRP and in the underlying masonry);
- No tensile and compression strength, respectively, for masonry and GFRP materials;
- The stress–strain constitutive law for the composite is based on the GFRP material alone, neglecting the mechanical contribution of the epoxy resin (due to fact that there is no strict control of the mixture process and its final thickness);
- Constitutive laws: parabolic for compressed masonry and linear elastic (up to failure) for GFRP reinforcement subjected to tension.

The former assumptions are similar to those that are commonly accepted for the computation of the ultimate flexural strength (with axial force) for reinforced concrete columns, the major difference being that in this case the compressive strength of the reinforcing material is neglected. The assumption that masonry behaves as a homogeneous material may be viewed as an approximation, even more than the similar assumption for concrete structural

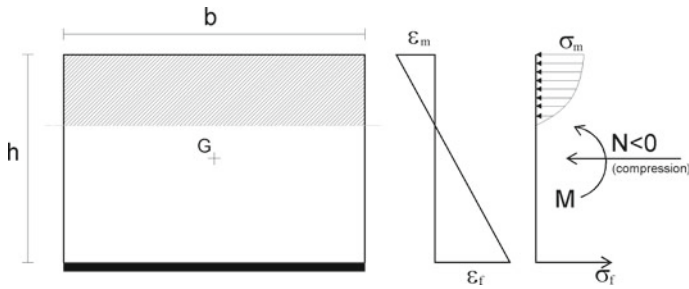


Fig. 18 Computation of the out-of-plane bending resistant moment: strain and stress diagrams (ϵ_m and σ_m represent the maximum compressive strain and stress on masonry and ϵ_f and σ_f the GFRP fibre tensile strain and stress)

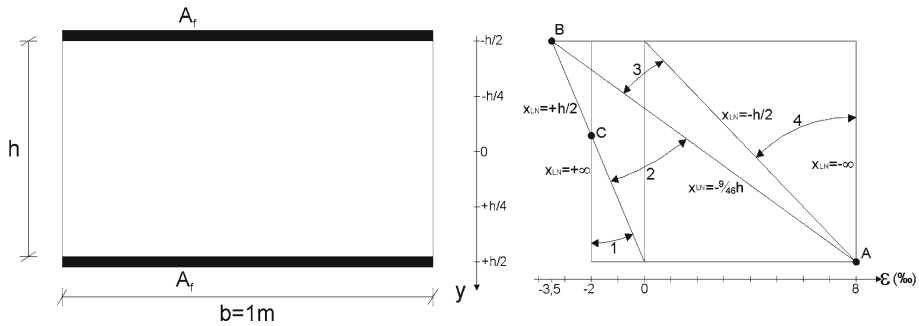


Fig. 19 Design zones covering all conventional failure strain diagrams. Failure Mode—Masonry crushing: Zone 1—Fully compressed cross section; Zone 2—Partially compressed cross section; Failure Mode—GFRP tensile fracture or debonding: Zone 3—Partially compressed cross section; Zone 4—Fully tensioned cross section

elements. Furthermore, the material constitutive laws were characterized by the following values: ultimate tensile strain of 8‰ for GFRP reinforcement; crushing strain of 2‰ (full compression) or 3.5‰ (compression and bending) and maximum strength of 2 MPa, for compressed masonry.

Figure 18 represents the normal stress and strain cross sectional distribution for a strengthened wall subjected to axial compression (N) and out of plane flexure (M). The internal forces N and M are computed by the integration of the normal stresses corresponding, through the constitutive laws, to the strain distribution along the cross section.

Cross section collapse can occur due to any of the following situations: masonry crushing and GFRP tensile fracture (or debonding), possibly due to anchorage failure. These two collapse situations correspond to four zones in terms of strain distribution along the cross section—zone 1–4, as depicted in Fig. 19. Masonry crushing comprises zone 1 (full compression) and zone 2 (partial compression), whereas GFRP tensile fracture (or debonding) comprises zone 3 (partial compression) and zone 4 (full tension). Zone 4 represents an unlikely failure mode for masonry walls, but was nevertheless considered to cover all theoretical situations.

The stress distribution, depicted in Fig. 18, and the cross-section strain distribution regions, depicted in Fig. 19, are also similar to those that are commonly accepted for the design of reinforced concrete columns.

Similarly to the design of reinforced concrete columns, the ultimate design bending moment and axial force combinations can be computed for each mechanical reinforcement

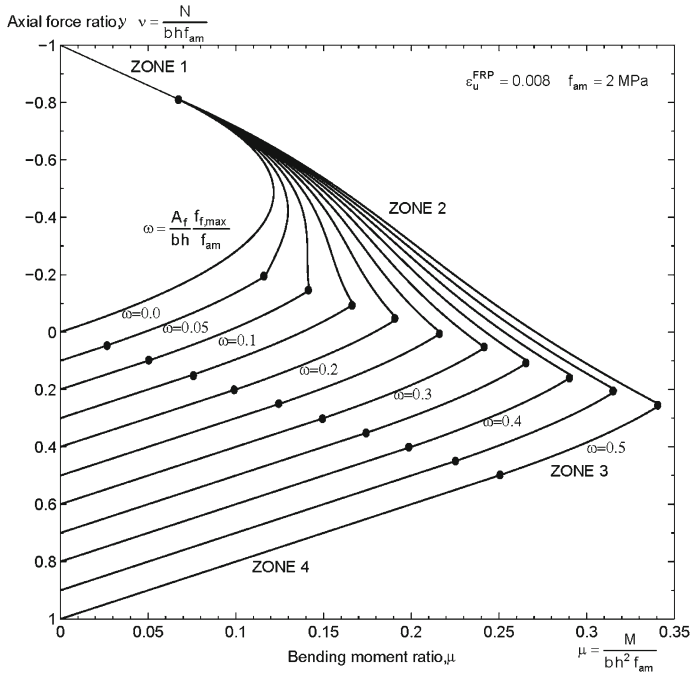


Fig. 20 Typical Design curve for masonry walls reinforced with the proposed technique

ratio value (ω), considering all possible limit situations (masonry crushing and GFRP tensile failure), as depicted in Fig. 20. Figure 20 also illustrates that, with the exception of highly compressed walls (axial force ratio $v < -0.5$), strengthening results in a significant increase in the bending capacity of the wall.

5 Conclusions

This paper presents a strengthening technique for traditional load-bearing stone masonry walls. The technique consists in the application of GFRP composite strips on masonry wall faces, bonded to the substrate and further connected to it through mechanical anchorages.

The strengthening technique was developed through an extensive series of experimental tests, which are briefly reviewed, composed by elementary material tests, medium scale tests on wall specimens and the application to a scaled building model.

The effectiveness of this technique is highly dependent on the capability of developing high stresses on the composite reinforcement, which, in turn, depends on bonding and anchorage effectiveness. For this reason a new experimental programme devoted to the study of interface bonding was conducted and is described in detail. An innovative test setup was developed, consisting in modifications carried out on the “beam test” configuration, with the use of a dummy steel block, thus leading to a reduction of the number of manufactured masonry blocks. A total number of 29 specimens were tested, varying, amongst other things, the number and spacing of anchorages. As a general conclusion of the experimental programme, it can be stated that the existence of anchorages proves to be highly beneficial in increasing the strength and deformation capacity of strengthened masonry walls. Tests have shown that

the strengthening technique is extremely effective, leading to high tensile stresses in the GFRP composite strips, which, in turn, led to premature failure modes in some of the tests. Specimens with multiple anchorages have shown higher deformation capacity than those with single anchorage. Maximum composite force showed no significant dependency on the anchorage spacing and a consistent decrease in strength in specimens subjected to cyclic load history was not identified. Increasing anchorage spacing may lead to debonding failure, whereas decreasing spacing leads to an increase in cost and workmanship. An intermediate spacing—in the order of magnitude of the wall thickness—is recommended.

A calculation model for the design of strengthened walls when subjected to combined compression and out of plane flexure is also presented. The proposed calculation model offers a rational attempt for consideration by engineers interested in out-of-plane upgrade of masonry walls with externally bonded GFRP composite strips with anchorages. Typical results obtained through the calculation model clearly show the effectiveness of the strengthening system, with a significant strength increase in moderately compressed walls.

References

- ACI (American Concrete Institute) (2007) Report on Fibre-Reinforced Polymer (FRP) reinforcement for concrete structures. Reported by ACI Committee 440 ACI 440R-07
- Campos-Costa A, Candeias P, Massena B (2001) Ensaios sísmicos de estruturas de alvenaria de pedra, 3ª Fase—Caracterização do comportamento de nembos em alvenaria de pedra reforçada para cargas repetidas e alternadas—Modelos M8, M9, M10 e M11—2ª Técnica de reforço. Report 244/01, LNEC, Lisbon, Portugal (in Portuguese)
- Candeias P, Campos-Costa A, Coelho E (2004) Shaking table tests of 1:3 reduced scale models of four story unreinforced masonry buildings. In: Proceedings of the 13th world conference on earthquake engineering. Vancouver, Canada
- Candeias P, Coelho E, Campos-Costa A (2006) Shaking table tests of 1:3 scale models of 4 stories URM buildings: model analysis and vulnerability assessment. In: Proceedings of the 1st European conference on earthquake engineering and seismology. Geneva, Switzerland
- Cardoso J (2008) Análise de uma solução de reforço sísmico de paredes de alvenaria tradicional com GFRP e ancoragens. Ensaios de aderência e modelo de cálculo. MSc thesis in Civil Engineering, IST TU Lisbon, Portugal (in Portuguese)
- Cardoso J, Proença J, Gago A, Cóias e Silva V, Paula R (2008) Development of a reduced intrusiveness seismic strengthening technique in traditional masonry walls through GFRP strips and anchorages. Bonding tests and design model. In: Proceedings of the international seminar on seismic risk and rehabilitation of stone masonry housing. Faial, Azores, Portugal
- Chen J, Yang Z, Holt G (2001) FRP or steel plate to concrete bonded joints: effects of test methods on experimental bond strength. *Steel Compos Struct* 1(2):231–244
- CML (Câmara Municipal de Lisboa) (2005) Diagnóstico Sócio-urbanístico da Cidade de Lisboa. Uma perspectiva censitária. Ed. Câmara Municipal de Lisboa, Lisbon, Portugal (in Portuguese)
- CNR (National Research Council) (2004) Guide for the design and construction of externally bonded FRP systems for strengthening existing structures: materials, RC and PC structures, masonry structures. CNR-DT 200/2004, Italy
- Cóias e Silva V (2001) Preserving baixa pombalina through low intrusive seismic rehabilitation methods—The COMREHAB Project. In: Proceedings of the international congress UNESCO-ICOMOS. Paris, France
- Cóias e Silva V (2007) Reabilitação Estrutural de Edifícios Antigos—Alvenaria, Madeira—Técnicas pouco intrusivas. Ed. Argumentum & Gecorpa, Lisbon, Portugal (in Portuguese)
- FIB (Fédération Internationale de Béton) (2001) Externally bonded FRP reinforcement for RC structures. Bulletin N. 14, Lausanne, Switzerland
- Gago A, Proença J, Cardoso J, Cóias V, Paula R (2009) Seismic strengthening of stone masonry walls with glass fibre reinforced polymer strips and mechanical anchorages. *Expe Tech Soc Exp Mech* (in press)
- ISO (International Organization for Standardization) (1993) Standard 527-1:1993: plastics—determination of tensile properties—part 1: general principles. Geneva, Switzerland
- ISO (International Organization for Standardization) (1997a) Standard 527-4:1997: plastics—determination of tensile properties—part 4: test conditions isotropic and orthotropic fibre-reinforced plastic composites. Geneva, Switzerland

- ISO (International Organization for Standardization) (1997b) Standard 527-5:1997: plastics—determination of tensile properties—part 5: test conditions for unidirectional fibre-reinforced plastic composites. Geneva, Switzerland
- Jifu L, Ming L, Yupu S (2007) Experimental investigation on flexural performance of masonry walls reinforced with GFRP. *J Wuhan Univ Technol Mater Sci Ed* 22(1):82–84
- Kiss RM, Jai J, Kollar LP, Krawinkler H (2002a) FRP strengthened masonry beams. Part I—model. *J Compos Mater* 36(5):521–536
- Kiss RM, Jai J, Kollar LP, Krawinkler H (2002b) Masonry strengthened with FRP subjected to combined bending and compression, part II—test results and model predictions. *J Compos Mater* 36(9):1049–1063
- LNEC (Laboratório Nacional de Engenharia Civil) (1993) E226 standard: Betão. Ensaio de compressão, Lisbon, Portugal (in Portuguese)
- S&P - Clever Reinforcement Company (2002) Design guide line for S&P FRP systems. Switzerland
- Tumialan JG, Galati N, Nanni A (2003) Fiber-reinforced polymer strengthening of unreinforced masonry walls subject to out-of-plane loads. *ACI Struct J* 100(3):321–329
- Yao J, Teng JG, Chen JF (2005) Experimental study on FRP-to-concrete bonded joints. *J Compos Part B Eng* 36(2):99–113